

# Unified Sand Model Based on the Critical State and Generalized Plasticity

Hoe I. Ling, M.ASCE<sup>1</sup>; and Songtao Yang<sup>2</sup>

**Abstract:** Based on the critical state concept and with the use of a state parameter, a unified generalized plasticity model is proposed for sand. The model uses a nonlinear critical state line. The plastic modulus, loading vectors and plastic flow direction vectors of a generalized plasticity model were modified so that they depend on the state parameter. With a single set of parameters, the model simulates the stress-deformation behavior of sand of different densities and pressure levels, under both drained and undrained conditions. A total of 12 parameters are required for monotonic loading and additional five parameters are included to consider cycling loading. The model is calibrated using the results of a minimum of two triaxial compression tests conducted on specimens of different densities and confining pressures. The model has been validated against the monotonic and cyclic test results of Toyoura sand, Nevada sand, and Fuji River sand. The comparison between simulations and test results showed that the model is capable of simulating sophisticated sand behavior. Its limitation in simulating monotonic loading following series of cyclic loadings of dense sand is discussed.

**DOI:** 10.1061/(ASCE)0733-9399(2006)132:12(1380)

**CE Database subject headings:** Sand; Plasticity; Parameters; Models.

## Introduction

The constitutive modeling of soil has achieved certain degree of success in the past several decades using different versions of elastoplastic formulations. The use of critical state concept has been rather successful for clay and models of different complexities have been proposed (e.g., Roscoe and Burland 1968; Schofield and Wroth 1968; Dafalias and Herrmann 1982; Ling et al. 2002). The modeling of sand remains a great challenge since sand behaves differently from clay. For example, it is well known that loose sand contracts while dense sand dilates under shearing. The use of critical state concept has not been popular for sand mainly because it cannot handle the dilatant behavior at the state dry of critical. In the models based on advanced plasticity, such as generalized plasticity (Pastor and Zienkiewicz 1986; Pastor et al. 1990), the same sand has to be treated as different materials depending on their density and pressure level because they behave differently under different states. As a result, a large number of soil parameters are required in analyzing the sand of varying densities when subjected to different confining pressures.

Casagrande (1936) proposed the concept of critical density of

soil. Roscoe et al. (1958) validated this concept, where the critical void ratio is independent of the stress path and drainage conditions, against experimental results obtained for several types of sands and clays. The critical state concept is basically identical to the steady state as of Poulos (1981) where deformation is considered to continue at constant volume, constant normal effective stress, constant shear stress, and constant rate of shear strain. Granta-gravel model (Schofield and Wroth 1968) was developed based on the critical state concept with a unique line of critical state in the  $p$ - $q$ - $e$  space. By comparing the theory with the experimental results of sands, good agreement was achieved only for very loose state sheared under drained conditions. Bardet (1986) developed a bounding surface model for sand based on the critical state concept. However, in his model, different critical state lines were assumed for the dense and loose sands. The critical state concept is further elaborated in the next section.

**State parameter and critical state line:** Realizing the fact that sand behavior is dependent on the pressure levels and densities, Been and Jefferies (1985) proposed a state parameter to account for these combined effects. The state parameter  $\psi$  gives the difference between existing and critical state values of void ratio at a given pressure

$$\psi = e - e_c \quad (1)$$

where  $e$ =existing void ratio and  $e_c$ =critical state void ratio. Thus, loose sand gives a positive value of  $\psi$  whereas for dense sand it is negative.

There were debates over the uniqueness of critical state line, such as the effects of stress path (Vaid et al. 1990) and initial void ratio (Yamamuro and Lade 1998). Been (1999) reexamined the test results of Yamamuro and Lade (1998) and indicated that the concept of critical state can practically be acceptable. However, different from clay, the critical state line for sands does not seem to be parallel to the normal compression line. Upon careful studies, a unique critical state line, which may become nonlinear over a wide range of pressure, was used. At large pressure, say beyond 1,000 kPa, breaking or crushing of soil grains may become sig-

<sup>1</sup>Associate Professor, Dept. of Civil Engineering and Engineering Mechanics, Columbia Univ., 500 West 120th St., New York, NY 10027; also, Visiting Associate Professor, Division of Engineering and Applied Sciences, Harvard Univ., 29 Oxford Street, Cambridge, MA 02138. E-mail: Ling@civil.columbia.edu

<sup>2</sup>Graduate Research Assistant, Dept. of Civil Engineering and Engineering Mechanics, Columbia Univ., 500 West 120th St., New York, NY 10027.

Note. Associate Editor: George Z. Voyiadjis. Discussion open until May 1, 2007. Separate discussions must be submitted for individual papers. To extend the closing date by one month, a written request must be filed with the ASCE Managing Editor. The manuscript for this paper was submitted for review and possible publication on April 11, 2005; approved on June 5, 2006. This paper is part of the *Journal of Engineering Mechanics*, Vol. 132, No. 12, December 1, 2006. ©ASCE, ISSN 0733-9399/2006/12-1380-1391/\$25.00.

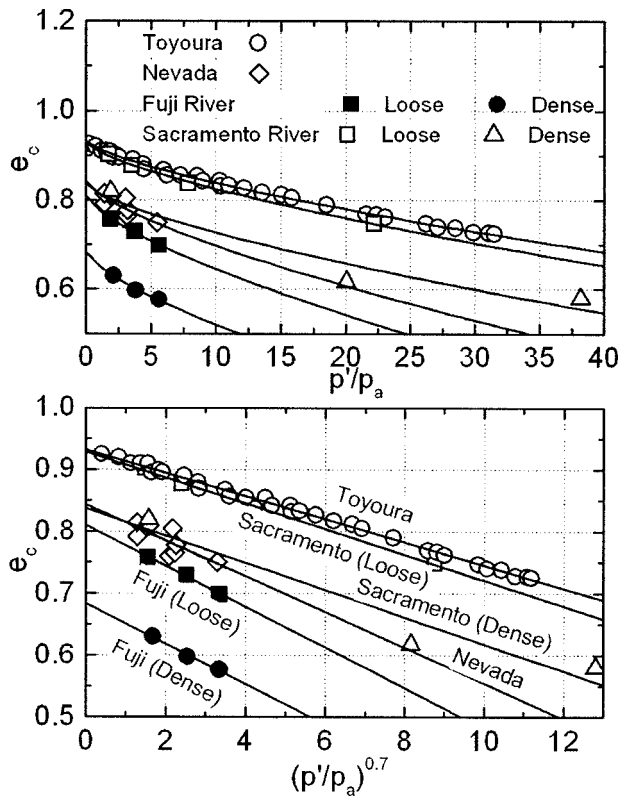


Fig. 1. Critical state line of sands

nificant (Been et al. 1991). Although a linear representation of  $e_c$ - $\log p'$  curve is acceptable for the pressure level encountered in practice, nonlinearities are considered by a few researchers.

Crouch et al. (1994) introduced a bilinear critical state line. Li and Wang (1998) suggested a nonlinear version of the critical state line, which may be expressed as follows:

$$e_c = e_{\Gamma} - \lambda_c \bar{p}^{\zeta} \quad (2)$$

where  $\bar{p} = p'/p_a$  = effective stress that is normalized by the atmospheric pressure,  $e_{\Gamma}$  and  $\lambda_c$  = intercept and slope of the critical state line in the  $e$  versus  $\bar{p}^{\zeta}$  plane, and  $\zeta$  = a constant.

Fig. 1 shows the critical state lines for four types of sands (Touyoua, Nevada, Fuji River, and Sacramento River) whose properties have been studied extensively. Three of these sands are used later to validate proposed constitutive model. The critical void ratio for Touyoua sand were presented by Verdugo and Ishihara (1996) and Ishihara (1996), whereas that of Nevada sand was from Yamamuro and Lade (1998), as compiled by Been (1999). Note that most of the triaxial test results for Nevada sand, as presented by Arulmori et al. (1992) for the VELACS project, did not reach the critical state. Lee and Seed (1967) studied Sacramento River sand under drained conditions and the results for Fuji River sand were presented by Tatsuoka (1972) and Tatsuoka and Ishihara (1974a,b). Li and Wang (1998) recommended  $\zeta$  to be 0.7 based on the results for two types of sand, including Touyoua sand. As shown in Fig. 1, although the range of pressure covered in the results of Fuji River sand and Nevada sand was not as wide as that of Touyoua and Sacramento River sands,  $\zeta = 0.7$  seems valid. Thus, Eq. (2) is conveniently written as

$$e_c = e_{\Gamma} - \lambda_c \bar{p}^{0.7} \quad (2')$$

There was a larger scattering of results for Nevada sand compared to Touyoua sand in fitting the nonlinear critical state line.

For Fuji River sand and Sacramento River sand, the critical state lines were not unique under the loose and dense states. It appears that the different methods of preparation of loose and dense specimens, i.e., pluviation versus vibration and tamping in the case of Fuji River sand, could have affected the uniqueness of the critical state line. In fact, the issue of preparation methods has recently been addressed by Papadimitriou et al. (2005). In addition, as the particle size increases, crushing of sand particles are more likely to occur. Of course, resistance against crushing depends also on the mineral compositions of the sands.

Under the same spirit as the state parameter, Ishihara (1993) proposed the state index, where the relative initial state of sand is considered. Instead of using void ratio as a state parameter, Wang et al. (2002) used pressure as a variable, termed state pressure index, which is defined as the ratio of current mean pressure to the mean pressure at the critical state corresponding to current void ratio. The unified models that are applicable to both sand and clay have also been proposed (e.g., Crouch et al. 1994; Pestana and Whittle 1999).

Several  $\psi$ -based sand models have been proposed in the literature. Nor-sand (Jefferies 1993) is a strain hardening model applicable to sand of very loose to very dense states. A bounding surface plasticity model was proposed by Manzari and Dafalias (1997) that accounted for the effects of pressure and density through a single set of parameters. Li et al. (1999) incorporated  $\psi$  into a bounding surface hypoplastic model to account for the sand behavior under different densities and pressure levels. These proposed models were valid for monotonic and cyclic loadings of sands under drained and undrained conditions.

In this paper, the concept of critical state was adopted through a state parameter, based on which the plastic modulus, loading vectors and plastic flow direction vectors of a generalized plasticity model were modified. The relationships between some of these quantities and the state parameters have been used successfully by several researchers in the past, such as Wood et al. (1994), Manzari and Dafalias (1997), Li and Dafalias (2000), and Wang et al. (2002). The proposed unified model was then used for the simulation of sand behavior under monotonic and cyclic loadings. The results obtained from simulations and experiments were compared.

## Proposed Model

The generalized plasticity model (Zienkiewicz and Mroz 1984; Mroz and Zienkiewicz 1984; Pastor et al. 1990) has gained considerable success in modeling the behavior of sand and soil structures, especially for cyclic loading. In the formulations, the yield or plastic potential surface and hardening rule are not specified directly, but the direction vectors are used. There have been several improvements made to the generalized plasticity model, as summarized in Ling and Liu (2003), to account for the complicated soil behavior that the original models could not handle. In Ling and Liu (2003), for example, the model was modified to consider the effects of pressure level and cyclic strain hardening. It, however, still suffered from the drawbacks of having to calibrate separately the same sand under different densities. That is, the model required extensive number of parameters for a single type of soil if variation of density is a concern.

In the generalized plasticity, the stress increment and strain increment vectors ( $d\sigma$  and  $d\epsilon$ ) are related through a elastoplastic matrix  $D_{ep}$ , similar to the classical elastoplasticity

$$d\sigma = D_{ep}d\varepsilon \quad (3a)$$

However, the elastoplastic matrix is expressed as

$$D_{ep} = D_e - \frac{D_e n_{gLU} n_{gLU}^T D_e}{H_{LU} + n_{gLU}^T D_e n_{gLU}} \quad (3b)$$

where  $D_e$ ,  $H_{LU}$ ,  $n$ , and  $n_{gLU}$  are the elastic matrix, plastic modulus, loading direction vectors, and plastic flow direction vectors, respectively. The subscripts  $L$  and  $U$  indicate loading and unloading, respectively.

Different from classical elastoplasticity, the yield and plastic potential surfaces are not directly specified in the generalized plasticity, but two scalar functions for the plastic modulus and three directions are needed. To incorporate the state parameters into generalized plasticity, the major plastic constituents of the model, such as dilatancy, plastic flow direction, and plastic modulus were modified accordingly, as described subsequently.

### Elastic Behavior

The elastic matrix comprised of two elastic constants. Typically, the shear modulus is an empirical relationship considering the effects of pressure level  $p'$  and void ratio  $e$  (e.g., Hardin and Richart 1963; Ishihara 1996)

$$G_{\max} = G_0 \frac{(2.97 - e)^2 \sqrt{p}}{1 + e} \quad (4a)$$

A similar relationship (Wang et al. 1990) for the bulk modulus is used

$$K_{\max} = K_0 \frac{(2.97 - e^2) \sqrt{p}}{1 + e} \quad (4b)$$

where  $G_0$  and  $K_0$  are the shear and bulk modulus numbers, respectively. In the model of Pastor et al. (1990), the shear modulus and bulk modulus are:  $G_{\max} = G_0 \bar{p}$  and  $K_{\max} = K_0 \bar{p}$ . In Eq. (4b), the Poisson's ratio is considered a constant when deriving for the bulk modulus. Note that the energy may not be conserved during cyclic loading based on above empirical equations for purely elastic materials (see Pestana and Whittle 1999). However, for elastoplastic material, the error can be minimum since the contribution of elastic behavior is very small with the deformation to be predominantly plastic. This argument was also made in Ling and Liu (2003) because the results would be erroneous for cyclic loading if the material is purely elastic.

### Dilatancy

The stress-dilatancy relationship proposed by Nova and Wood (1979) has been used in the different versions of generalized plasticity model. The dilatancy  $d_g$  and stress ratio  $\eta = q/p'$  are related as follows:

$$d_g = (1 + \alpha)(M_g - \eta) \quad (5a)$$

where  $M_g$ =slope of the critical state line in the  $p'$ - $q$  plane and  $\alpha$ =parameter. At the critical state,  $\eta = M_g$  and thus  $d_g$  equal to zero.

The model was originally formulated in the triaxial stress space, but it has then been extended into three-dimensional stress space by considering the third invariants (Lode's angle  $\theta$ ) in  $M_g$

$$M_g = \frac{6 \sin \phi'_g}{3 - \sin \phi'_g \sin 3\theta} \quad (5b)$$

where  $\phi'_g$ =angle of internal friction at the critical state.

It is clear that Eq. (5a) is not valid for sand of different densities. For instance, during shearing, dense sand first contracts and then reaches a state of phase transformation where the volume change is zero. It then dilates and finally reaches the critical state with zero volume change. On the other hand, a loose sand contracts and reaches the critical state upon shearing, while the phase transformation is not observed. Thus, the same stress ratio may imply dilation for dense sand and contraction for loose sand.

In the dense sand, the phase transformation angle in the  $p'$ - $q$  plane is dependent on the pressure level; the slope at the phase transformation  $M_d$  increases with an increase in the pressure level as observed by Manzari and Dafalias (1997) and Li and Dafalias (2000). Manzari and Dafalias (1997) used a linear relationship to express the dependency of  $M_d$  on  $\psi$ , whereas Li and Dafalias (2000) used the exponential relationship:  $M_d = M_g \exp(m_g \psi)$ , where  $m_g$ =positive constant.

Following Li and Dafalias (2000), Eq. (5a) is modified in this study to give dilatancy as

$$d_g = (1 + \alpha)(M_d - \eta) \quad (6a)$$

$$M_d = M_g \exp(m_g \psi) \quad (6b)$$

where  $m_g$ =constant. Eq. (6a) satisfies the criteria of critical state where the volume change equal to zero for  $\psi=0$  and  $\eta=M_d$ . For an initially dense sand ( $\psi < 0$ ), the phase transformation state is reached when  $\eta = M_g \exp(m_g \psi')$ , where  $\psi'$ =value of  $\psi$  at the phase transformation state. For an initially loose sand ( $\psi > 0$ ),  $M_d = M_g \exp(m_g \psi) > M_g$  and thus, the phase transformation state is never reached during the course of shearing.

### Plastic Flow

In generalized plasticity, the plastic flow direction vector  $n_{gL}$  and the loading direction vectors  $n$  are expressed as follows:

$$n_{gL} = \left( \frac{d_g}{\sqrt{1 + d_g^2}}, \frac{1}{\sqrt{1 + d_g^2}} \right)^T \quad (7a)$$

$$n = \left( \frac{d_f}{\sqrt{1 + d_f^2}}, \frac{1}{\sqrt{1 + d_f^2}} \right)^T \quad (7b)$$

In the original model,  $d_f$  is a loading direction vector which is expressed as

$$d_f = (1 + \alpha)(M_f - \eta) \quad (8)$$

where  $M_f$ =constant with the ratio  $M_f/M_g$ =relative density. Ling and Liu (2003) shows that for Toyoura sand,  $M_f$  increases with an increase in the void ratio  $e$ . Thus, the following function is adopted:

$$d_f = (1 + \alpha)(M_h - \eta) \quad (9a)$$

$$M_h = M_f \exp(m_f(1 - e)) \quad (9b)$$

where  $M_f$  and  $m_f$ =constants. For sand where  $M_h$  is insensitive to the change in void ratio,  $m_f$  is set as zero such that Eq. (9a) degenerates to Eq. (8). For three-dimensional stress conditions,  $M_f$  is extended using a similar function as Eq. (5b).

It has to be noted that using the loading and unloading direction vectors, one has the convenience of obtaining a distinction

between loading and unloading, as well as the definition of neutral loading. Neutral loading, however, implies that one can bring the stress state from triaxial compression to triaxial extension without any plastic deformation that is in contradiction to the experimental results.

### Loading Plastic Modulus

In the original model, the loading plastic modulus  $H_L$  is expressed as

$$H_L = H_0 p' H_f \left( 1 - \frac{\eta}{M_g} + \beta_0 \beta_1 \exp(-\beta_0 \xi) \right) \quad (10a)$$

$$H_f = \left( 1 - \frac{\eta}{\eta_f} \right)^4 \quad (10b)$$

$$\eta_f = \left( 1 + \frac{1}{\alpha} \right) M_f \quad (10c)$$

where  $H_0$ ,  $\beta_0$ , and  $\beta_1$  are constants.  $\xi = \int |d\epsilon_s^p|$  = accumulative plastic deviatoric strain and  $H_f$  = plastic coefficient.

Several modifications are made to the plastic modulus with a new expression, which is dependent on the square root of effective stress and the state parameter:

$$H_L = H_0 \sqrt{p} H_f (M_b - \eta) / \eta \quad (11)$$

where  $H_f$  = same function as the original model, and  $H_0$  and  $M_b$  = functions of the void ratio and state parameter, respectively

$$H_0 = H_{L0} \exp(m_0(1 - e)) \quad (12a)$$

$$M_b = M_g \exp(-m_b \psi) \quad (12b)$$

Here,  $H_{L0}$ ,  $m_0$ , and  $m_b$  are constants. When  $H_0$  is insensitive to the initial void ratio,  $m_0 = \text{zero}$ . The linear dependence of  $M_b$  on  $\psi$  was proposed by Wood et al. (1994) and has been used by Manzari and Dafalias (1997):  $M_b = M_g - m_g \psi$ , whereas Li and Dafalias (2000) has the same expression as Eq. (12b).

As can be seen in Eq. (11), the value of  $H_L$  depends on the difference between current stress ratio  $\eta$  and "virtual" peak stress ratio  $M_b$ .  $H_L$  may be positive (for  $M_b > \eta$ , hardening), negative (for  $M_b < \eta$ , softening) or zero (for  $M_b = \eta$ , peak or failure).

### Plastic Moduli under Cyclic Loading

The loading plastic modulus is modified to consider cyclic loading. In addition, the unloading and reloading moduli are incorporated.

### Loading/Reloading Modulus

The test results on sands under drained conditions showed that significant modulus reduction may occur during the first cycle of unloading, and thus a factor  $\beta_r$  is included in  $H_0$ . In addition, sands show densification behavior when subjected to repeated loading under drained conditions. The densification factor  $H_{\text{den}}$ , which is a function of the total volumetric strain  $\epsilon_v$ , is incorporated into the modulus. Thus, for undrained conditions where the total volumetric strain is zero, the densification factor does not affect the modulus.

Considering above-mentioned effects, the reloading modulus is now expressed as

$$H_L = \beta_r H_{\text{den}} H_0 \sqrt{p} H_f (M_b - \eta) / \eta \quad (13a)$$

$$H_{\text{den}} = \exp(-r_{\text{den}} \epsilon_v) \quad (13b)$$

$$\beta_r = \left( 1 + \frac{1}{\alpha} + \frac{\eta}{M_g} \right)^{-\kappa} \quad (13c)$$

where  $H_{\text{den}}$  = densification factor;  $\beta_r$  = modulus degradation factor;  $r_{\text{den}}$  and  $\kappa$  = constants.

When the stress states reach the phase transformation line, the plastic modulus decreases rapidly such that the state parameter alone is inadequate for simulating the cyclic behavior. In order to consider cyclic behavior such as liquefaction and cyclic mobility of loose and dense sands, respectively, a function of plastic deviatoric strain is included in  $M_b$  to account for possible modulus degradation

$$M_b = M_g \exp(m_c \psi) \quad (14a)$$

$$m_c = m_g - (m_g + m_b) \exp(-\beta \xi) \quad (14b)$$

where  $\beta$  = positive parameter and  $\xi$  = accumulated plastic deviatoric strain.

$m_c$  changes from  $-m_b$  to  $m_g$  as  $\xi$  changes from zero to infinity. That is, as  $\xi$  increases,  $H_L$  will approach zero when  $\eta = M_d$  (i.e.,  $d_g = 0$ ) at the phase transformation line. Different from monotonic loading,  $\psi$  may not approach zero under undrained cyclic loading, and that is why  $M_b$  is expressed in such a way that not only  $d_g$  but also  $H_L$  will approach zero when  $\eta = M_d$ . In fact, the expression  $m_c$  allows the model to recalculate  $\xi$  from a new origin of values during at any stage of loading, similar to if one has continued to use the first origin of values for  $\xi$ . The use of  $\xi$ , however, may have a negative effect in simulating monotonic loading following a series of cyclic loadings, as discussed under the section: Limitations of model.

### Unloading Modulus

The unloading plastic modulus  $H_U$  of the original model is used, but a new control factor of unloading is introduced. The factor is based on the ratio  $|M_d / \eta_U|$  instead of  $|M_g / \eta_U|$  as in the original model since the critical state line is dependent on the state parameter. The densification factor of Eq. (13b) is also introduced into the modulus

$$H_U = H_{\text{den}} H_{U0} \sqrt{p} \left( \frac{M_g}{\eta_U} \right)^{m_U} \quad \text{for } |M_d / \eta_U| > 1 \quad (15a)$$

$$H_U = H_{\text{den}} H_{U0} \quad \text{for } |M_d / \eta_U| \leq 1 \quad (15b)$$

where  $H_{U0}$  and  $m_U$  = parameters and  $\eta_U$  = stress ratio for unloading to take place. The control factor allows unloading modulus to be  $H_{U0}$  if loading starts at a point of dilative behavior ( $d_g < 0$ ) or at the phase transformation state ( $d_g = 0$ ).

The plastic strain develops during unloading, but of contractive nature. Thus the flow direction vector under unloading is expressed as

$$n_{gU} = \left( -\text{abs} \left( \frac{d_g}{\sqrt{1 + d_g^2}} \right), \frac{1}{\sqrt{1 + d_g^2}} \right)^T \quad (16)$$

### Calibration of Model

The proposed model requires a total number of 12 parameters for monotonic loading and 17 parameters when cyclic loading is considered. They are the elastic parameters ( $G_0, K_0$ ), and parameters

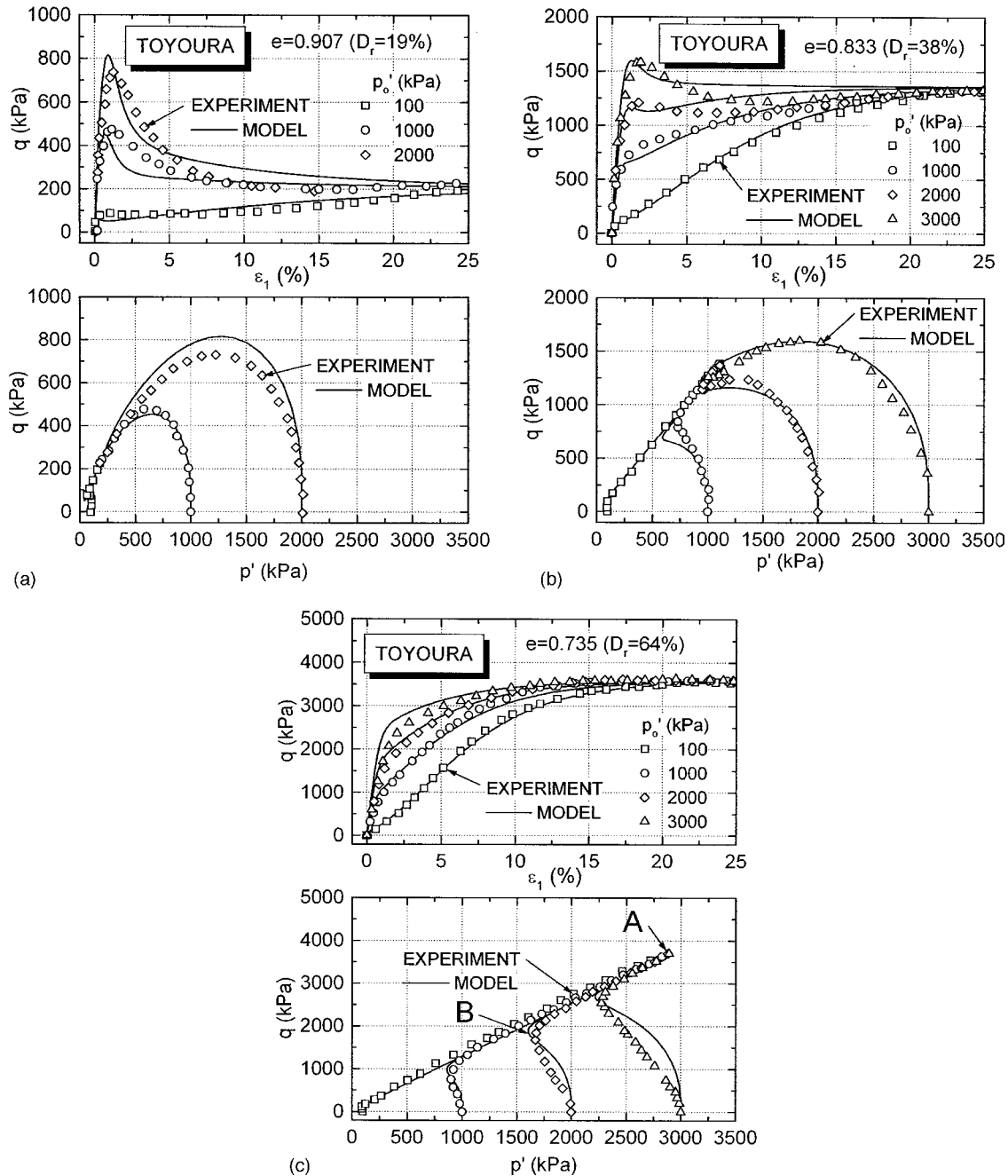


Fig. 2. Comparison of Toyoura sand under undrained monotonic loading: (a)  $e=0.907$ ; (b)  $e=0.833$ ; and (c)  $e=0.735$

related to the critical state line ( $e_T, \lambda_c$ ), dilatancy ( $\alpha, M_g, m_g$ ), plastic flow ( $M_f, m_f$ ), loading modulus ( $m_0, H_{L0}, m_b$ ), unloading modulus ( $H_{U0}, m_U$ ), and unloading/reloading modulus ( $\beta, r_{den}, \kappa$ ). This number of parameters seems required for advanced models, such as Li et al. (1999), that consider salient features of soil behavior including cyclic loading. Most parameters have definite physical meaning although a few of them, mainly the cyclic parameters, are obtained by best fitting the experimental results. The exponents  $m_g, m_f, m_b$  may be assumed as zero in certain cases. For this model, drained or undrained tests of different densities and pressures (a minimum of two) are required to determine the monotonic parameters. To include cyclic behavior, a cyclic loading test is required. Note that although step by step procedures are described in determining the parameters, optimization scheme (Mattsson et al. 2001; Yang and Elgamal 2003) may be used.

The two parameters of the critical state line  $e_T$  and  $\lambda_c$ , are obtained from  $e_c - \log p'$  relationship or through a linear curve between  $e_c$  and  $(p'/p_a)^{0.7}$  (Fig. 1). A minimum of two tests having different initial densities that cover the range of void ratio of interest are required. The specimens are sheared at either drained or undrained conditions up to the critical state.

The determination of elastic parameters is straight forward.  $G_0$  and  $K_0$  define the elastic behavior of sand.  $G_0$  is obtained from the stress-strain curve or from the elastic wave propagation tests in the field or laboratory, such as the Bender test. Triaxial tests with small strain measurement may also be used to quantify the elastic shear modulus (e.g., Tatsuoka and Shibuya 1991).  $K_0$  can be obtained from isotropic compression test or by matching the initial slope of  $\varepsilon_1$  versus  $p'$  or  $\varepsilon_v$  versus  $p'$  curve.

The parameter  $m_g$  can be determined from either drained or

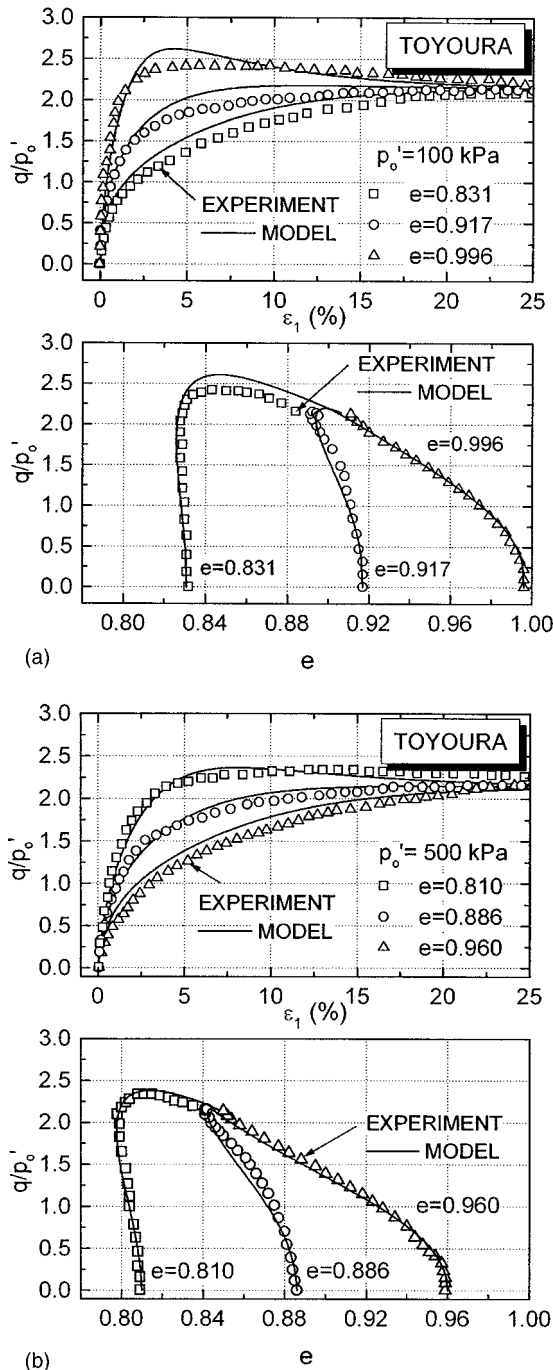


**Fig. 3.** Comparison of Toyoura sand under drained monotonic loading: (a)  $p' = 100$  kPa; (b)  $p' = 500$  kPa

undrained tests by evaluating Eq. (6b) at a phase transformation state, at which  $d_g = 0$ . Hence,

$$m_g = \frac{1}{\psi_d} \ln \frac{M_d}{M_g} \quad (17)$$

where  $M_d$  and  $\psi_d$  = values of  $\eta$  and  $\psi$  at the phase transformation state. Also, the parameter  $m_g$  can be obtained by directly matching the phase transformation point for drained or undrained tests. Typical range of value of  $m_g$  is from 0.5 to 3.

The parameter  $m_b$  can be obtained from Eq. (12b) at a drained peak stress ratio, at which  $H_L = 0$ . Hence,

**Table 1.** Parameters of Unified Generalized Plasticity Model

| Model properties   | Parameters   | Toyourea sand | Nevada sand | Fuji River sand               |
|--|--------------|---------------|-------------|-------------------------------|
| Elastic moduli   | $G_0/p_a$    | 450           | 450         | 210                           |
|  | $K_0/p_a$    | 450           | 450         | 210                           |
| Critical state line  | $e_T$        | 0.934         | 0.843       | 0.81 (loose)<br>0.684 (dense) |
|  | $\lambda_c$  | 0.019         | 0.0287      | 0.033                         |
| Phase transformation line  | $M_g$        | 1.25          | 1.35        | 1.49                          |
|  | $m_g$        | 3.0           | 1.0         | 2.5                           |
| Plastic flow   | $M_f$        | 0.21          | 1.2         | 0.52                          |
|  | $m_f$        | 6.5           | 0.0         | 1.65                          |
| Loading modulus  | $H_{L0}/p_a$ | 110           | 2160        | 200                           |
|  | $m_b$        | 6             | 1.37        | 3.91                          |
|  | $m_0$        | 2             | 1.0         | 4.0                           |
| Constant related to dilatancy, flow direction, and loading modulus | $\alpha$     | 0.1           | 0.45        | 0.45                          |
|  | $H_{U0}/p_a$ | 340           | 300         | 288                           |
| Unloading modulus  | $m_U$        | 3.3           | 3.6         | 2.0                           |
|  | $\beta$      | 50            | 80          | 11.5                          |
| Reloading modulus  | $\kappa$     | -1.9          | 0.0         | -1.4                          |
|  | $r_{den}$    | 180           | 8.0         | 130                           |

$$m_b = \frac{1}{\psi_b} \ln \frac{M_g}{M_b} \quad (18)$$

where  $M_b$  and  $\psi_b$  = values of  $\eta$  and  $\psi$  at the drained peak stress state. Also, the parameter  $m_b$  can be determined by directly matching the ratio of peak stress to residual stress in the strain-stress curve for drained tests. Typical range of value of  $m_0$  is from 0.5 to 3.

For the parameter  $\alpha$ , ignoring the small elastic deformations in the drained tests,  $d_g$  is obtained from Eq. (6)

$$\frac{d\varepsilon_v}{d\varepsilon_q} \approx \frac{d\varepsilon_v^p}{d\varepsilon_q^p} = d_g = (1 + \alpha)[M_g \exp(m_g \psi) - \eta] \quad (19)$$

So, the parameter  $\alpha$  can be calibrated using the  $\varepsilon_v - \varepsilon_q$  curves. It is typically set as 0.45 (e.g., Pastor et al. 1990; Ling and Liu 2003).

In determining  $M_f$ ,  $m_f$ ,  $H_{L0}$ , and  $m_0$ , it is more convenient to look at the values  $M_h = M_f \exp(m_f(1-e))$ —Eq. (9b) and  $H_0 = H_{L0} \exp(m_0(1-e))$ —Eq. (12a) as two combined entities through the two drained or undrained tests conducted at different initial densities.  $M_h$  can be determined by matching the shape of the monotonic stress-strain curve in the undrained tests or  $\varepsilon_v$  versus  $\varepsilon_1$  curve in the drained tests, whereas  $H_0$  can be determined by fitting both the monotonic stress-strain curve and  $\varepsilon_v$  versus  $\varepsilon_1$  curve for drained tests or the  $p' - q$  stress path for undrained tests.  $M_h$  may vary very little with density, in which  $m_f$  can be set to zero. After having fitted for one density,  $M_h$  is used for the first trial on the fitting for other value(s) of density.  $M_f$  is typically between 0.2 and 1.3, which is smaller than  $M_g$ , and the value of  $H_0$  is comparable with the values of  $G_0$  and  $K_0$ . The looser is the sand, the smaller the values of  $M_f$  and  $H_0$  become.

### Example of Model Calibration

To illustrate the calibration of 12 parameters for monotonic loading, the following two triaxial compression tests of Toyoura

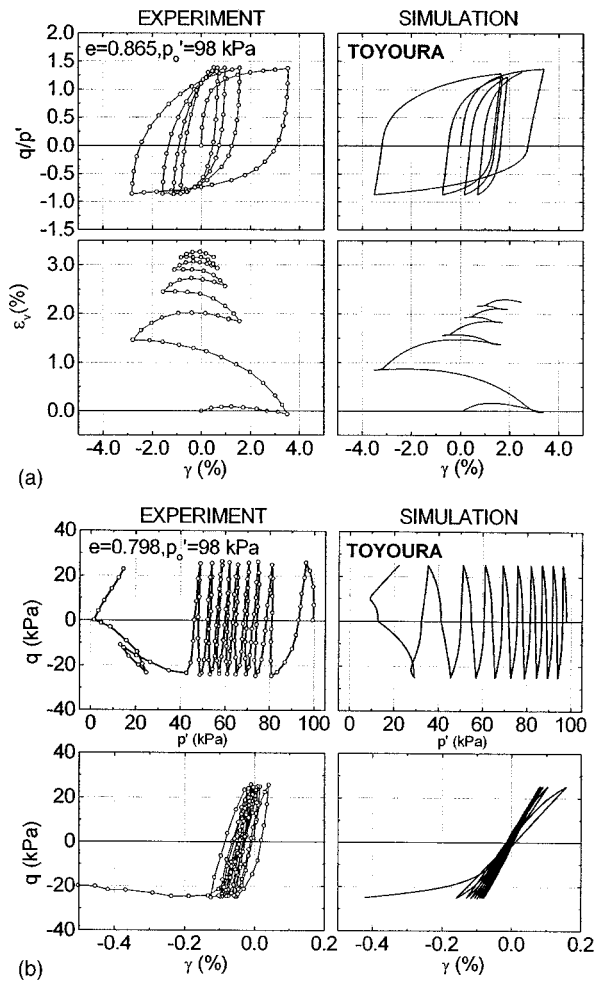


Fig. 4. Comparison of Toyoura sand under cyclic loading: (a) drained; (b) undrained

sand of Verdugo and Ishihara (1996) are used: undrained test with  $e=0.735$  and  $p'=2000$  kPa and drained test with  $e=0.886$  and  $p'=500$  kPa.

The relationship between the critical state void ratio and effective stress (Fig. 1) gives  $e_c=0.934-0.019(p'/p_a)^{0.7}$ . Thus,  $e_T=0.934$  and  $\lambda_c=0.019$ , where  $p_a=100$  kPa. The elastic parameters  $G_0$  and  $K_0$  are obtained from the literature as 45,000 kPa.

Referring to Fig. 2(c), Point A shows the critical state with  $p'=3,612$  kPa and  $q=2,880$  kPa. So, the slope of line OA gives  $M_g=2,880/3,612=1.25$ . Point B indicates the phase transformation ( $p'=1,600$  kPa,  $q=1,635$  kPa). So, the stress ratio at phase transformation  $M_d=1,635/1,600=1.022$ , and the corresponding state parameter  $\psi_d=0.735-\{0.934-0.019(1,600/100)^{0.7}\}=-0.0669$ . From Eq. (17),

$$m_g = \frac{1}{\psi_d} \ln \frac{M_d}{M_g} = \frac{1}{(-0.0669)} \ln \left( \frac{1.022}{1.25} \right) = 3.0$$

Then, set  $\alpha$  as 0.45 (a typical value),  $n$  in the range of 0.5–3.0,  $M_f$  in the range of 0.3 to  $M_g=1.25$ , and  $H_0$  to be comparable with  $G_0$  or  $K_0$ , in order to have the first trial on the experimental results. Based on the calibration procedure as mentioned earlier, through trial and error, the following values of parameters are obtained:  $m_0=2.0$ ,  $\alpha=0.1$ ,  $M_h=0.72$ , and  $H_0=3.4 \times 10^4$  for the first test [see Fig. 2(c)]. For the second test,  $M_h=1.2$  and  $H_0=5.4 \times 10^4$  [Fig. 3(b)]. After substituting the values of  $M_h$  and

corresponding  $e$  into  $M_h=M_f \exp(m_f(1-e))$ ,  $M_f$  and  $m_0$  were determined by solving simultaneously a set of linear equations. Similarly,  $H_{L0}$  and  $m_0$  were determined by substituting the values of  $H_0$  and corresponding  $e$  into  $H_0=H_{L0} \exp(m_0(1-e))$ . The parameters were obtained as  $M_f=0.21$ ,  $m_f=6.5$ ,  $H_{L0}=1.1 \times 10^4$ , and  $m_0=6.0$ .

There are five additional parameters required to describe the cyclic behavior.  $H_{u0}$  is determined by simulating the initial slope of the first unloading curve;  $m_u$  is determined from the rate of change of the slope of the first unloading curve or through the number of cycles in cyclic test. An increased value of  $H_{u0}$  and  $m_u$  leads to a stiffer response and thus more loading cycles for the stress path to reach the phase transformation line.  $\kappa$  is determined from the slope of the first reloading curve or through the number of cycles in the cyclic test. An increased value leads to a softer reloading curve.  $\beta$  is obtained from the hysteretic loops in the stress-strain curve. It has a significant effect on the stress-strain response after the stress path reaches the phase transformation line, but not before reaching the line. An increased value in  $\beta$  resulted in rapid modulus degradation. Experimental results for calibration should include appropriate stress amplitude if degradation is to be accounted for.  $r_{den}$  is determined by simulating the hysteretic loops in the stress-strain curve under drained cyclic loading. An increased value of which resulted in a more pronounced cyclic hardening. The parameters for Toyoura sand are summarized in Table 1.

The effects of model parameters on the stress-strain response are studied in Yang (2005).

## Model Validation

The results from three types of sand are used to validate the model: Toyoura sand, whose calibration procedure has been illustrated earlier, Nevada sand, and Fuji River sand. Toyoura sand has been studied extensively by different researchers in Japan. Here, the series of triaxial compression test results from Verdugo and Ishihara (1996) and Pradhan (1989) are used for the calibration and validation of the model under monotonic and cyclic loadings. The results of Verdugo and Ishihara (1996) cover a wide range of pressure and void ratios. Nevada sand was used in the VELACS project and the results of Arulmori et al. (1992) and Yamamuro and Lade (1998) are used for calibration of the model. Fuji River sand (Tatsuoka 1972) has been used in validating many cyclic models in the literature. The parameters used for the model are summarized in Table 1 for the three types of sand.

### Toyourea Sand

Two series of drained and three series of undrained triaxial compression tests were conducted by Verdugo and Ishihara (1996). The specimens were prepared using moist placement method. In the drained tests, two different confining pressures of 100 and 500 kPa were used for the specimens having three different void ratios, ranging from 0.81 to 0.996.

The procedures used to determine the 12 monotonic parameters were illustrated earlier. Figs. 2(a and b) show the results of simulation compared with the experimental results in terms of the stress ratio versus axial strain ( $q/p'_0-\epsilon_1$ ) and stress ratio versus void ratio ( $q/p'_0-e$ ) relationships. In both cases, the simulations show that the stress-strain relationships converged to a critical state value. The overall soil behavior is well expressed by the model.

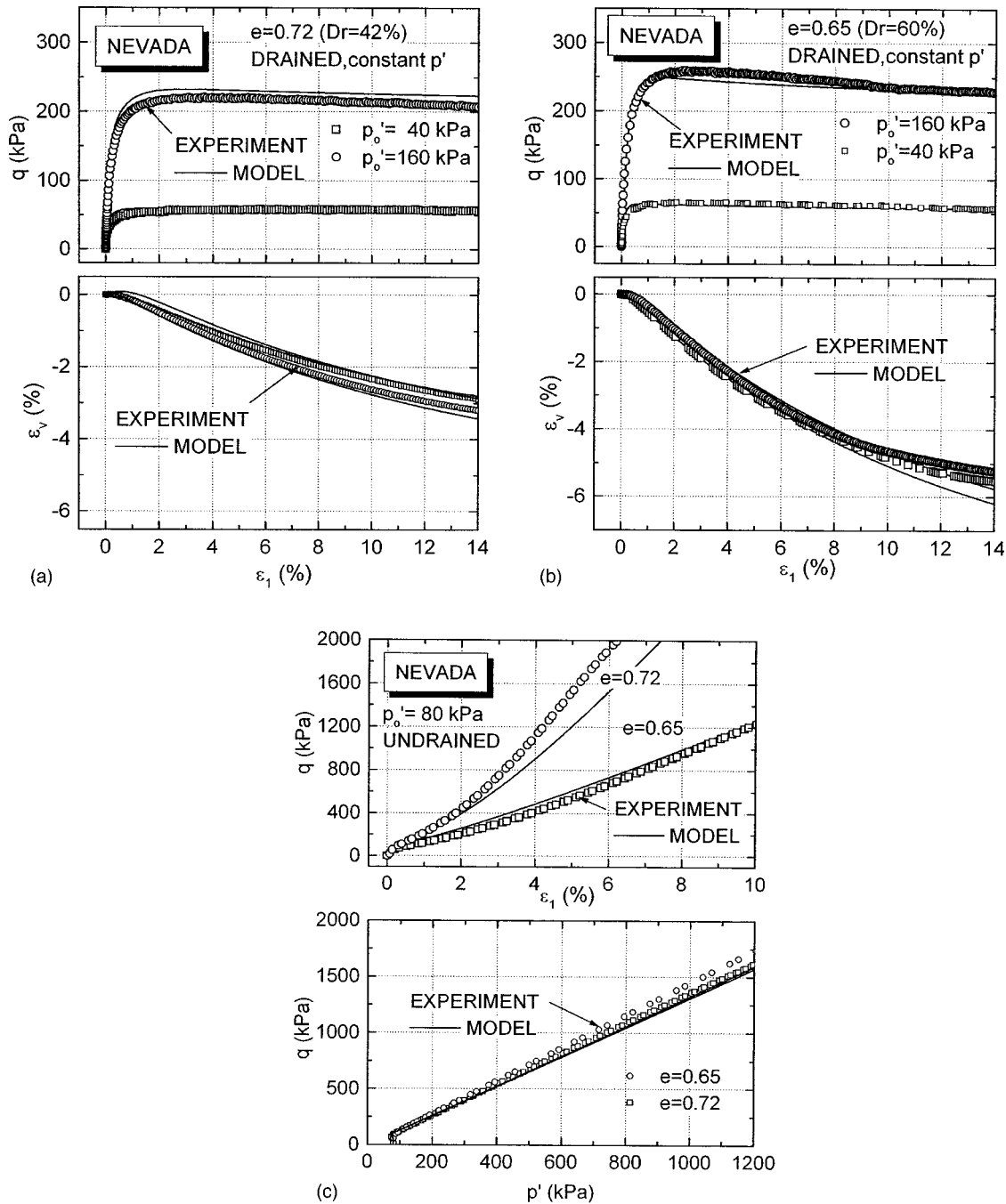


**Fig. 5.** Comparison of Nevada sand under monotonic loading: (a) drained  $e=0.72$ ; (b) drained  $e=0.65$ ; and (c) undrained  $p'_o=80$  kPa

The undrained tests were conducted at a confining pressure ranging from  $p=100$  to  $3,000$  kPa at three different void ratios ( $e=0.735, 0.833$ , and  $0.907$ ) that corresponded to a relative density of 16, 38, and 64%, respectively. Figs. 3(a–c), show the results of simulation compared with the test results in terms of deviator stress versus axial strain ( $q-\epsilon_1$ ) relationships and the effective stress path ( $q-p'$ ). It is seen that the strain hardening and softening behavior, together with the critical state, are well depicted in the simulations.

The additional five parameters relevant for cyclic loading were calibrated from the cyclic test results of Pradhan (1989). The results of calibration/simulation for the drained ( $e=0.865$ ,  $p'=98$  kPa) and undrained tests ( $e=0.798$ ,  $p'=98$  kPa, stress amplitude  $q=\pm 25$  kPa) are shown in Figs. 4(a and b), respectively.

Note, however that the Toyoura sand used by Pradhan (1989) was of a different batch from Verdugo and Ishihara (1996), thus the index properties were slightly different. Despite the slight difference in properties, the results showed that the cyclic behavior, especially the cyclic hardening, was simulated by the model. As the stress amplitude is large, the reduction in modulus following the first reloading, compared to first loading, is simulated. The model was also able to simulate the cyclic behavior under undrained loading until onset of liquefaction.

### Nevada Sand

The triaxial test results of Arulmori et al. (1992) were used for calibration and the results of simulation were compared. The

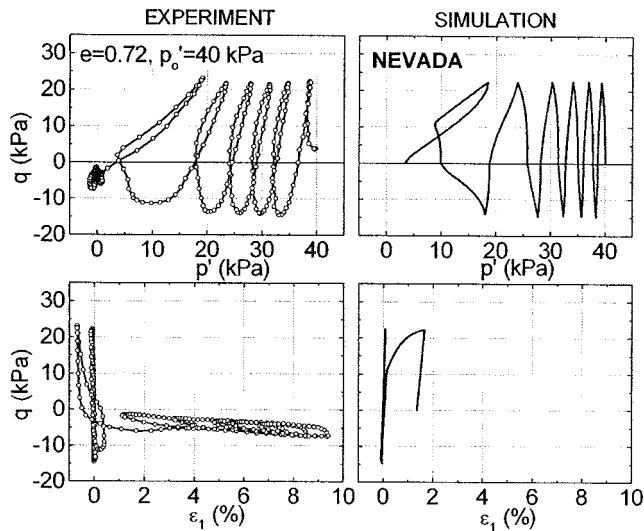


**Fig. 6.** Comparison of Nevada sand under undrained cyclic loading:  $e=0.72$  and  $p'=40$  kPa

Nevada test specimens were prepared by dry pluviation method. Note that the critical state parameters were based on Yamamuro and Lade (1998) as shown in Fig. 1 since the tests of Arulmori et al. (1992) did not reach the critical state.

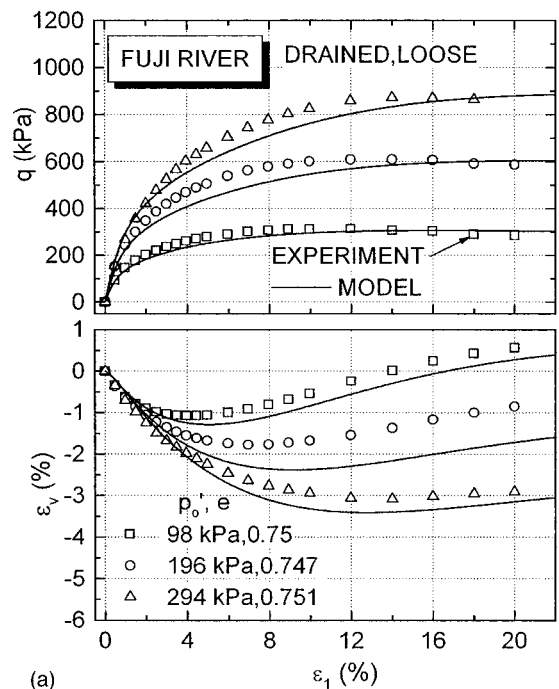
The calibration was conducted based on the two series of drained  $p'$ -constant tests for relative densities of 40% ( $e=0.72$ ) and 60% ( $e=0.65$ ) at a constant effective stress of  $p'=40$  and 160 kPa [Figs. 5(a and b)].  $p'$ -constant series of tests were selected because they were conducted for both drained and undrained conditions, but not the conventional triaxial compression tests. The calibrated model was used to predict the behavior of undrained triaxial compression tests for the two relative densities at  $p'=80$  kPa [Fig. 5(c)]. In general, the comparison yielded satisfactory results.

Two cyclic triaxial undrained tests were also predicted and compared. One of the cyclic tests was conducted at  $e=0.72$  and  $p'=40$  kPa with  $q=-14.5-22.3$  kPa, whereas the other test was conducted at  $e=0.65$  and  $p'=80$  kPa with  $q=-22.1-37.1$  kPa. The cyclic tests were load controlled using a sinusoidal wave of frequency 1 Hz. The comparison for the stress paths yielded satisfactory results. Due to space limitation, only the former is shown in Fig. 6. However, for the deviator stress–axial strain relationships, the excessively large axial displacement could not be predicted well after onset of liquefaction.

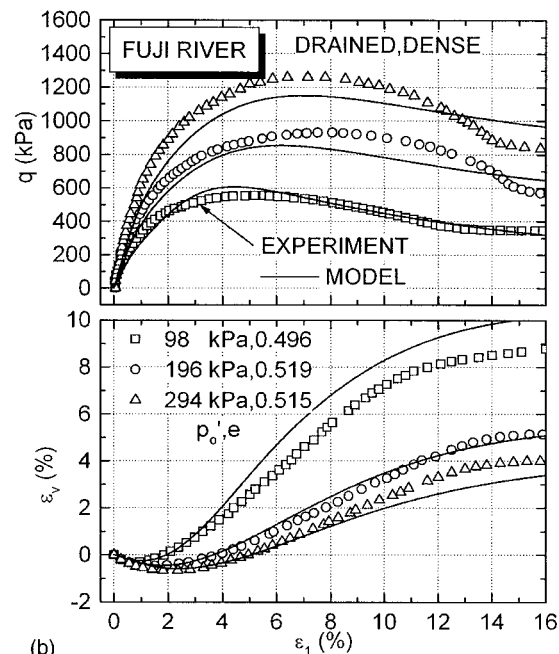
### Fuji River Sand

The behavior of Fuji River sand has been studied by Tatsuoka (1972) and Tatsuoka and Ishihara (1974a,b) for different stress paths and loading conditions, both monotonic and cyclic loadings. The test results have been used by many researchers in validating constitutive models (such as Nova 1982; Bardet 1986; Pastor et al. 1990; Ling and Liu 2003). Specimens of different densities and confining pressures were used. In the validation, only the loose ( $e=0.80$ ,  $D_r=51\%$ ) and dense ( $e=0.54$ ,  $D_r=92\%$ ) states were considered under triaxial compression. The loose specimens were prepared by pluviation method, whereas the dense specimens were prepared by vibration and tamping.

Similar to Toyoura and Nevada sand, the model was first calibrated against the drained test results of loose and dense specimens covering three different confining pressures ranging from 98



(a)



(b)

**Fig. 7.** Comparison of Fuji River sand under drained monotonic loading: (a) loose; (b) dense

to 294 kPa [Figs. 7(a and b)]. Note that as the critical state for the loose and dense conditions is not unique, which could be due to the methods of specimen preparation as discussed earlier, two different critical state parameters were used (Fig. 1). The other material parameters are the same for the loose and dense states that interestingly did not affect significantly the accuracy of simulation under drained and undrained conditions [Figs. 8(a and b)].

The model is then used to simulate drained cyclic loading behavior. First, the loose specimen is simulated with stress amplitude that increased with cycles of loading. The increase in volumetric strain with cycles of loading is described by the model [Fig. 9(a)]. To investigate the cyclic hardening behavior of sand,

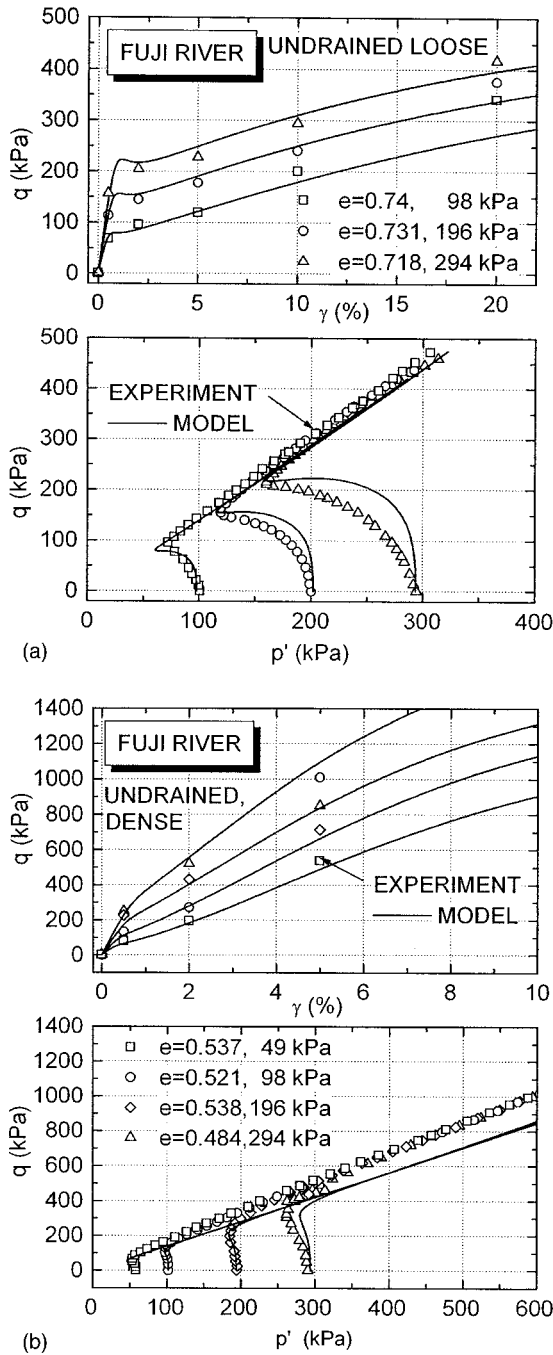


**Fig. 8.** Comparison of Fuji River sand under undrained monotonic loading: (a) loose; (b) dense

the loose sand is simulated for cycles of loading under constant stress amplitude. As can be seen in Fig. 9(b), the model showed a reduction in the rate of volume change with the loading cycles.

The behavior of Fuji River sand under undrained cyclic loading is simulated for the loose and dense states. At loose state, the strain controlled tests of constant stress amplitudes were considered. Fig. 10 shows the results of simulation where the stress paths of the experimental results and simulation gave reasonable agreement prior to liquefaction. The stress-strain behavior is less favorable as the strain level increased. The simulations for stress controlled test on loose and dense specimens of varying stress amplitude are given in Yang (2005).

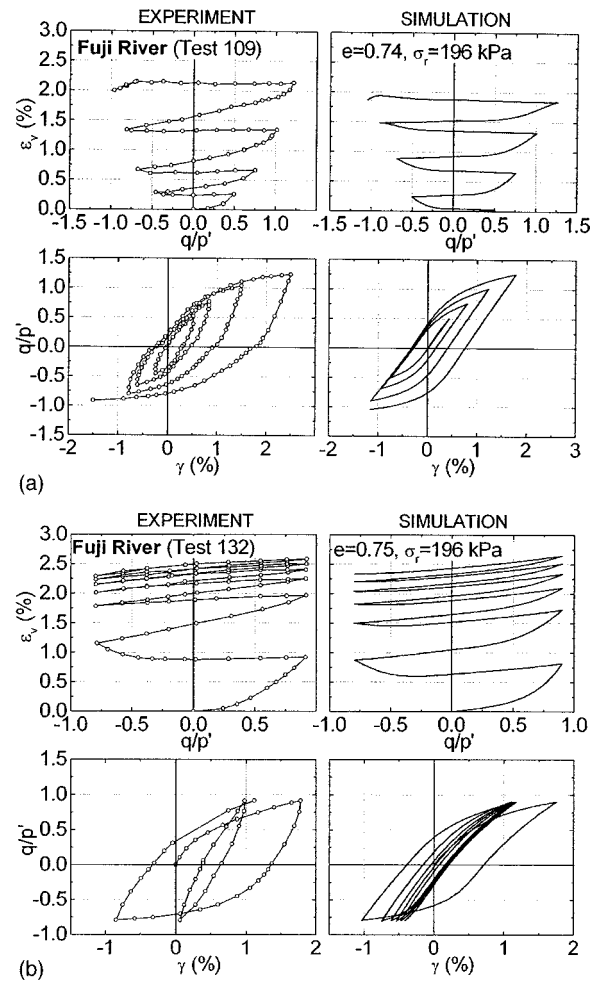


**Fig. 9.** Comparison of Fuji River sand under drained cyclic loading: (a) varying stress amplitude; (b) constant stress amplitude

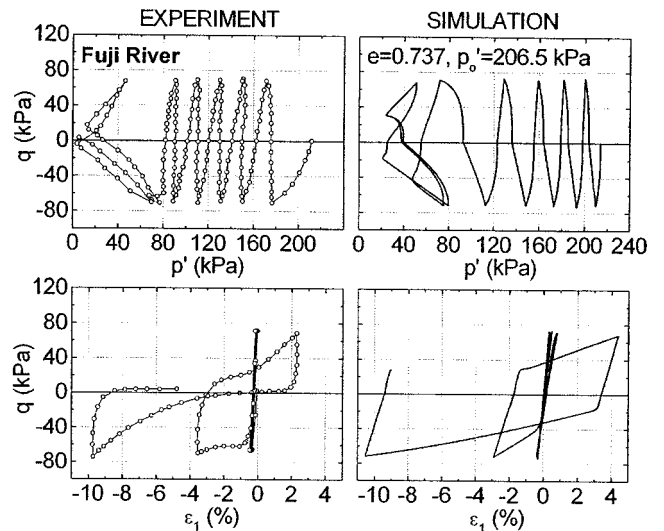


**Fig. 10.** Comparison of Fuji River sand under undrained cyclic loading

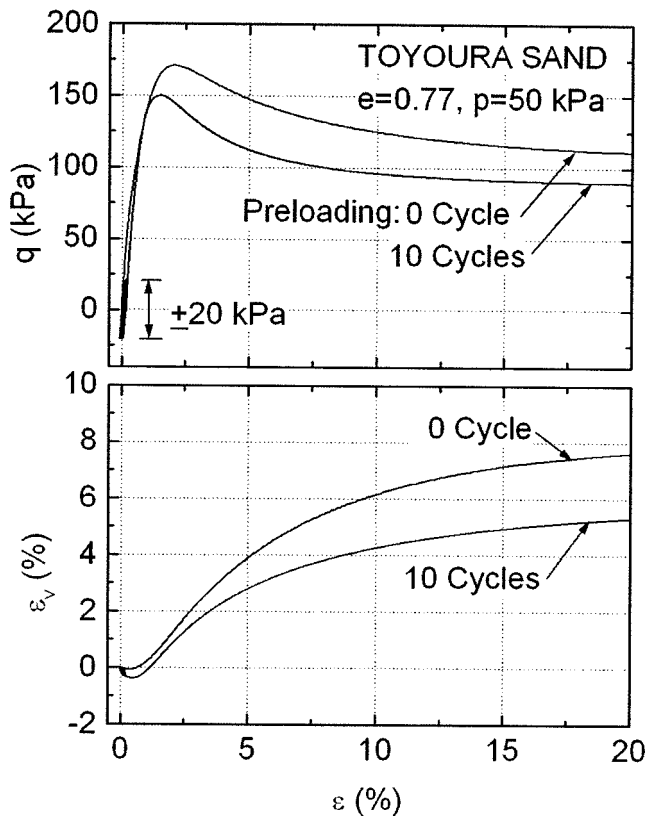


**Fig. 11.** Simulation of stress-strain response of dense Toyoura sand subjected to previous loading cycles

### Limitations on Cyclic-Monotonic Loading Response

The use of  $\xi$  induces non-reversible effects due to the monotonic increase in its value. Since there is no way that  $\xi$  will decrease ever, the effect it has on  $m_c$  via Eq. (14b) is permanent. Although  $m_c$  which changes from  $-m_b$  to  $m_g$  will effect the virtual peak stress ratio  $M_b$  in such a way that will be helping to control the cyclic accumulation of strain in drained tests or pore water pressure in undrained tests, it may yield unacceptable monotonic loading response.

Consider a dense specimen (negative  $\psi$ ). According to Eqs. (14a) and (14b), with  $\xi=0$  initially,  $m_c=-m_b$  thus resulting in  $M_b > M_g$ . This implies that if one loads the specimen monotonically in drained loading, the stress-strain curve will show the characteristic stress ratio rising above  $M_g$  toward  $M_b$  (the developing  $\xi$  will not be large enough to have any appreciable effects), and subsequent softening toward  $M_g$  at critical failure. Assume now that the previous specimen is submitted to cyclic drained loading of rather small amplitude. A light consolidation takes place since the stress ratio will not increase above the phase transformation value of  $M_d$  to induce dilation, but the deviatoric strain will keep accumulating even after the density has been stabilized [see, e.g., Fig. 9(b)]. This implies that  $\xi$  will keep increasing and as a result Eq. (14b) will render  $m_c=m_g$ , while Eq. (14a) will make  $M_b=M_g \exp(m_g\psi)$ , which with  $\psi$  negative will imply that  $M_b < M_g$  as if the specimen was loose.

Although the use of  $\xi$  shows benefit in the cyclic loading simulation, it may have a undesirable outcome if one submits a cyclically loaded dense specimen to monotonic loading. To illustrate this negative effect, Fig. 11 shows the comparison of the stress-strain response of the dense Toyoura sand that has not been and

has been subjected to ten cycles of loading. The results show that subsequent strength in monotonic loading dropped with previous loading cycles. Thus, caution should be taken in simulating monotonic loading following cyclic loading, to ensure that the previous number of loading cycles was small. The results are affected by the parameter  $\beta$ . The difference in the deformation behavior of the two simulations show the accumulated plastic strain under cyclic loadings.

### Summary and Conclusions

A model based on generalized plasticity and critical state concept has been proposed to describe the pressure dependency of sand behavior under different initial densities and drainage conditions. The model was unified over a wide range of densities and confining pressures in the sense that a single set of parameters were used to simulate the behavior. The model also described the cyclic loading behavior. By comparing the results of simulation with the experimental results, it is shown that

- The model simulated the contractive and dilative behavior of sand under loose and dense states, respectively. It also showed that the stress state converged to a critical state when sheared to large strain.
- The effects of pressure on the response of initially loose and dense sands were well depicted by the model using a single set of parameters for both drained and undrained shearings.
- The behavior of sand under cyclic loading, that is liquefaction for undrained conditions and cyclic hardening for drained conditions, was simulated by the model. However, for dense sand, the simulation of monotonic loading following cyclic loadings has to be done with care, perhaps limited to the conditions of small number of loading cycles.

The constitutive model is incorporated into the finite element procedure for the static and cyclic response analyses of geotechnical structures.

### Acknowledgments

The study is based upon works supported by the National Science Foundation under Career Award Grant No. CMS-0092739 with Dr. Richard J. Fragaszy as Program Director. The development of unified model was inspired by the comments made by one of the reviewers for Ling and Liu (2003). In the current submission, the anonymous reviewer provided useful insights into generalized plasticity and issues related to cyclic loading simulation.

### References

- Arulmori, K., Muraleetharan, K. K., Hossain, M. M., and Fruth, L. S. (1992). *VELACS Laboratory Testing Program, Soil Data Rep.*, Earth Technology Corporation, Irvine, Calif.
- Bardet, J. P. (1986). "Bounding surface plasticity model for sands." *J. Eng. Mech.*, 112(11), 1198–1217.
- Been, K. (1999). "The critical state line and its application to soil liquefaction." *Physics and mechanics of soil liquefaction*, P. V. Lade and J. A. Yamamuro, eds., Balkema, Rotterdam, The Netherlands, 195–204.
- Been, K., and Jefferies, M. G. (1985). "A state parameter for sand." *Geotechnique*, 35(2), 99–112.
- Been, K., Jefferies, M. G., and Hachev, J. (1991). "The critical state of

- sands." *Geotechnique*, 41(3), 365–381.
- Casagrande, A. (1936). "Characteristics of cohesionless soils affecting the stability of slopes and earth fills." *J. Boston Soc. Civ. Eng.*, 23(1), 13–32.
- Crouch, R. S., Wolf, J. P., and Dafalias, Y. F. (1994). "Unified critical-state bounding-surface plasticity model for soil." *J. Eng. Mech.*, 120(11), 2251–2270.
- Dafalias, Y. F., and Herrmann, L. R. (1982). "Bounding surface formulation of soil plasticity." *Soil mechanics-transient and cyclic loads*, G. N. Pande and O. C. Zienkiewicz, eds., Wiley and Sons, New York, 253–311.
- Hardin, B. O., and Richart, F. E. (1963). "Elastic wave velocities in granular soils." *J. Soil Mech. and Found. Div.*, 89(1), 33–65.
- Ishihara, K. (1993). "Liquefaction and flow failure during earthquakes." *Geotechnique*, 43(3), 351–415.
- Ishihara, K. (1996). *Soil behavior in earthquake geotechnics*, Oxford University Press, New York.
- Jefferies, M. G. (1993). "Nor-sand: A simple critical state model for sand." *Geotechnique*, 43(1), 91–103.
- Lee, K. L., and Seed, H. B. (1967). "Drained strength characteristics of sands." *J. Soil Mech. and Found. Div.*, ASCE, 93(SM6), 117–141.
- Li, X. S., and Wang, Y. (1998). "Linear representation of steady-state line for sand." *J. Geotech. Geoenviron. Eng.*, 124(12), 1215–1217.
- Li, X. S., and Dafalias, Y. F. (2000). "Dilatancy for cohesionless soils." *Geotechnique*, 50(4), 449–460.
- Li, X.-S., Dafalias, Y. F., and Wang, Z.-L. (1999). "State-dependent dilatancy in critical-state constitutive modeling of sand." *Can. Geotech. J.*, 36(4), 599–611.
- Ling, H. I., and Liu, H. (2003). "Pressure-level dependency and densification behavior of sand through a generalized plasticity model." *J. Eng. Mech.*, 129(8), 851–860.
- Ling, H. I., Yue, D., Kaliakin, V., and Themelis, N. J. (2002). "Anisotropic elastoplastic bounding surface model for cohesive soils." *J. Geotech. Geoenviron. Eng.*, 128(7), 748–758.
- Manzari, M. T., and Dafalias, Y. F. (1997). "A critical state two-surface plasticity model for sands." *Geotechnique*, 47(2), 255–272.
- Mattsson, H., Klisinski, M., and Axelsson, K. (2001). "Optimization routine for identification of model parameters in soil plasticity." *Int. J. Numer. Analyt. Meth. Geomech.*, 25(5), 435–472.
- Mroz, Z., and Zienkiewicz, O. C. (1984). "Uniform formulation of constitutive equations for clay and sand." *Mechanics of engineering materials*, C. S. Desai and R. H. Gallagher, eds., Wiley, New York, 415–450.
- Nova, R. (1982). "A constitutive model for soil under monotonic and cyclic loading." *Soil mechanics-transient and cyclic loading*, G. N. Pande and O. C. Zienkiewicz, eds., Wiley, New York, 343–373.
- Nova, R., and Wood, D. M. (1979). "A constitutive model for sand in triaxial compression." *Int. J. Numer. Analyt. Meth. Geomech.*, 3(3), 255–278.
- Papadimitriou, A. G., Dafalias, Y. F., and Yoshimine, M. (2005). "Plasticity modeling of the effect of sample preparation method on sand response." *Soils Found.*, 40, 109–124.
- Pastor, M., and Zienkiewicz, O. C. (1986). "A generalized plasticity, hierarchical model for sand under monotonic and cyclic loading." *Proc., 2nd Int. Symp. on Numerical Models in Geomechanics*, 131–150.
- Pastor, M., Zienkiewicz, O. C., and Chan, A. H. C. (1990). "Generalized plasticity and the modeling of soil behavior." *Int. J. Numer. Analyt. Meth. Geomech.*, 14(3), 151–190.
- Pestana, J. M., and Whittle, A. J. (1999). "Formulation of a unified constitutive model for clays and sands." *Int. J. Numer. Analyt. Meth. Geomech.*, 23, 1215–1243.
- Poulos, S. J. (1981). "The steady state of deformation." *J. Geotech. Engrg. Div.*, 107(5), 553–562.
- Pradhan, T. B. S. (1989). "The behavior of sand subjected to monotonic and cyclic loadings." Ph.D. thesis, Kyoto Univ., Kyoto, Japan.
- Roscoe, K. H., and Burland, J. B. (1968). "On the generalized strain-strain behavior of wet clay." *Engineering plasticity*, J. Heyman and F. A. Leckie, eds., Cambridge University Press, Cambridge, U.K., 535–609.
- Roscoe, K. H., Schofield, A. N., and Wroth, C. P. (1958). "On the yielding of soils." *Geotechnique*, 8(1), 22–53.
- Schofield, A. N., and Wroth, C. P. (1968). *Critical state soil mechanics*, McGraw-Hill, London.
- Tatsuoka, F. (1972). "A fundamental study of the behavior of sand by triaxial testing. Doctoral thesis, University of Tokyo, Tokyo, Japan.
- Tatsuoka, F., and Ishihara, K. (1974a). "Yielding of sand in triaxial compression." *Soils Found.*, 14(2), 63–76.
- Tatsuoka, F., and Ishihara, K. (1974b). "Drained deformation of sand under cyclic stresses reversing direction." *Soils Found.*, 14(3), 51–65.
- Tatsuoka, F., and Shibuya, S. (1991). "Deformation characteristics of soils and rocks from field and laboratory tests." *Proc., 9th Asian Regional Conf. on Soil Mechanics and Foundation Engineering*, Bangkok, 101–1077.
- Vaid, Y. P., Chung, E. K. F., and Kuerbis, R. H. (1990). "Stress path and steady state." *Can. Geotech. J.*, 27(1), 1–7.
- Verdugo, R., and Ishihara, K. (1996). "The steady state of sandy soils." *Soils Found.*, 36(2), 81–91.
- Wang, Z.-L., Dafalias, Y. F., Li, X.-S., and Makdisi, F. I. (2002). "State pressure index for modeling sand behavior." *J. Geotech. Geoenviron. Eng.*, 128(6), 511–519.
- Wang, Z.-L., Dafalias, Y. F., and Shen, C. K. (1990). "Bounding surface hypoplasticity model for sand." *J. Eng. Mech.*, 116(5), 983–1001.
- Wood, M. D., Belkheir, K., and Liu, D. F. (1994). "Strain softening and state parameter for sand modeling." *Geotechnique*, 44(2), 335–339.
- Yamamuro, J. A., and Lade, P. V. (1998). "Steady-state concepts and static liquefaction of silty sands." *J. Geotech. Geoenviron. Eng.*, 124(9), 868–877.
- Yang, S. (2005). "A unified plasticity model and its application to geotechnical analysis." Doctoral thesis, Columbia Univ., New York.
- Yang, Z., and Elgamal, A. (2003). "Application of unconstrained optimization and sensitivity analysis to calibration of a soil constitutive model." *Int. J. Numer. Analyt. Meth. Geomech.*, 27(15), 1277–1297.
- Zienkiewicz, O. C., and Mroz, Z. (1984). "Generalized plasticity formulation and applications to geomechanics." *Mechanics of Engineering Materials*, C. S. Desai and R. H. Gallagher, eds., Wiley, New York, 655–679.